

## 2.4 Paraxial Wave Equation and Gaussian Beams

So far, we have only treated optical systems operating with plane waves, which is an idealization. In reality plane waves are impossible to generate because of their infinite amount of energy required to do so. The simplest (approximate) solution of Maxwell's equations describing a beam of finite size is the Gaussian beam. In fact many optical systems are based on Gaussian beams. Most lasers are designed to generate a Gaussian beam as output. Gaussian beams stay Gaussian beams when propagating in free space. However, due to its finite size, diffraction changes the size of the beam and lenses are employed to reimage and change the cross section of the beam. In this section, we want to study the properties of Gaussian beams and its propagation and modification in optical systems.

### 2.4.1 Paraxial Wave Equation

We start from the Helmholtz Equation (2.18)

$$(\Delta + k_0^2) \tilde{\vec{E}}(x, y, z, \omega) = 0, \quad (2.214)$$

with the free space wavenumber  $k_0 = \omega/c_0$ . This equation can easily be solved in the Fourier domain, and one set of solutions are of course the plane waves with wave vector  $|\vec{k}|^2 = k_0^2$ . We look for solutions which are polarized in  $x$ -direction

$$\tilde{\vec{E}}(x, y, z, \omega) = \tilde{E}(x, y, z) \vec{e}_x. \quad (2.215)$$

We want to construct a beam with finite transverse extent into the  $x$ - $y$ -plane and which is mainly propagating into the positive  $z$ -direction. As such we may try a superposition of plane waves with a dominant  $z$ -component of the  $k$ -vector, see Figure 2.56. The  $k$ -vectors can be written as

$$\begin{aligned} k_z &= \sqrt{k_0^2 - k_x^2 - k_y^2}, \\ &\approx k_0 \left( 1 - \frac{k_x^2 - k_y^2}{2k_0^2} \right). \end{aligned} \quad (2.216)$$

with  $k_x, k_y \ll k_0$ .

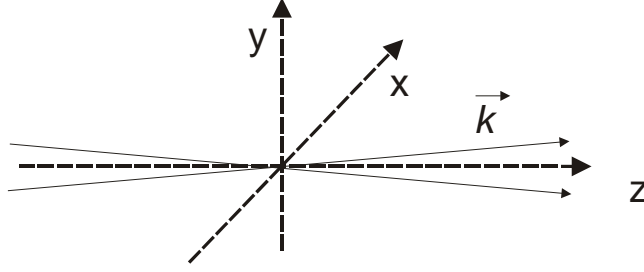


Figure 2.56: Construction of a paraxial beam by superimposing many plane waves with a dominant  $k$ -component in  $z$ -direction.

Then we obtain for the propagating field

$$\begin{aligned}
 \tilde{E}(x, y, z) &= \int_{-\infty}^{+\infty} \int_{-\infty}^{+\infty} \tilde{E}_0(k_x, k_y) \cdot \\
 &\quad \exp \left[ -jk_0 \left( 1 - \frac{k_x^2 + k_y^2}{2k_0^2} \right) z - jk_x x - jk_y y \right] dk_x dk_y, \\
 &= \int_{-\infty}^{+\infty} \int_{-\infty}^{+\infty} \tilde{E}_0(k_x, k_y) \cdot \\
 &\quad \exp \left[ j \left( \frac{k_x^2 + k_y^2}{2k_0} \right) z - jk_x x - jk_y y \right] dk_x dk_y e^{-jk_0 z}, \quad (2.217)
 \end{aligned}$$

where  $\tilde{E}_0(k_x, k_y)$  is the amplitude for the waves with the corresponding transverse  $k$ -component. This function should only be nonzero within a small range  $k_x, k_y \ll k_0$ . The function

$$\tilde{E}_0(x, y, z) = \int_{-\infty}^{+\infty} \int_{-\infty}^{+\infty} \tilde{E}_0(k_x, k_y) \exp \left[ j \left( \frac{k_x^2 + k_y^2}{2k_0} \right) z - jk_x x - jk_y y \right] dk_x dk_y \quad (2.218)$$

is a slowly varying function in the transverse directions  $x$  and  $y$ , and it can be easily verified that it fulfills the paraxial wave equation

$$\frac{\partial}{\partial z} \tilde{E}_0(x, y, z) = \frac{-j}{2k_0} \left( \frac{\partial^2}{\partial x^2} + \frac{\partial^2}{\partial y^2} \right) \tilde{E}_0(x, y, z). \quad (2.219)$$

Note, that this equation is in its structure identical to the dispersive spreading of an optical pulse. The difference is that this spreading occurs now in the two transverse dimensions and is called diffraction.

### 2.4.2 Gaussian Beams

Since the kernel in Eq.(2.218) is quadratic in the transverse  $k$ -components using a two-dimensional Gaussian for the amplitude distribution leads to a beam in real space which is also Gaussian in the radial direction because of the resulting Gaussian integral. By choosing for the transverse amplitude distribution

$$\tilde{E}_0(k_x, k_y) = \exp \left[ -\frac{k_x^2 + k_y^2}{2k_T^2} \right], \quad (2.220)$$

Eq.(2.218) can be rewritten as

$$\tilde{E}_0(x, y, z) = \int_{-\infty}^{+\infty} \int_{-\infty}^{+\infty} \exp \left[ j \left( \frac{k_x^2 + k_y^2}{2k_0} \right) (z + jz_R) - jk_x x - jk_y y \right] dk_x dk_y, \quad (2.221)$$

with the parameter  $z_R = k_0/k_T^2$ , which we will later identify as the Rayleigh range. Thus, Gaussian beam solutions with different finite transverse width in  $k$ -space and real space behave as if they propagate along the  $z$ -axis with different imaginary  $z$ -component  $z_R$ . Carrying out the Fourier transformation results in the Gaussian Beam in real space

$$\tilde{E}_0(x, y, z) = \frac{j}{z + jz_R} \exp \left[ -jk_0 \left( \frac{x^2 + y^2}{2(z + jz_R)} \right) \right]. \quad (2.222)$$

The Gaussian beam is often formulated in terms of the complex beam parameter or  $q$ -parameter.

The propagation of the beam in free space and later even through optical imaging systems can be efficiently described by a proper transformation of the  $q$ -parameter

$$\tilde{E}_0(r, z) = \frac{1}{q(z)} \exp \left[ -jk_0 \left( \frac{r^2}{2q(z)} \right) \right]. \quad (2.223)$$

Free space propagation is then described by

$$q(z) = z + jz_R \quad (2.224)$$

Using the inverse  $q$ -parameter, decomposed in real and imaginary parts,

$$\frac{1}{q(z)} = \frac{1}{R(z)} - j \frac{\lambda}{\pi w^2(z)}. \quad (2.225)$$

leads to

$$\tilde{E}_0(r, z) = \frac{\sqrt{2P}}{\sqrt{\pi}w(z)} \exp \left[ -\frac{r^2}{w^2(z)} - jk_0 \frac{r^2}{2R(z)} + j\zeta(z) \right]. \quad (2.226)$$

Thus  $w(z)$  is the waist of the beam and  $R(z)$  is the radius of the phase fronts. We normalized the beam such that the Gaussian beam intensity  $I(z, r) = \left| \tilde{E}_0(r, z) \right|^2$  expressed in terms of the power  $P$  carried by the beam is given by

$$I(r, z) = \frac{2P}{\pi w^2(z)} \exp \left[ -\frac{2r^2}{w^2(z)} \right], \quad (2.227)$$

$$\text{i.e. } P = \int_0^\infty \int_0^{2\pi} I(r, z) r dr d\varphi. \quad (2.228)$$

The use of the  $q$ -parameter simplifies the description of Gaussian beam propagation. In free space propagation from  $z_1$  to  $z_2$ , the variation of the beam parameter  $q$  is simply governed by

$$q_2 = q_1 + z_2 - z_1. \quad (2.229)$$

where  $q_2$  and  $q_1$  are the beam parameters at  $z_1$  and  $z_2$ .

If the beam waist, at which the beam has a minimum spot size  $w_0$  and a planar wavefront ( $R = \infty$ ), is located at  $z = 0$ , the variations of the beam spot size and the radius of curvature of the phase fronts are explicitly expressed as

$$w(z) = w_0 \left[ 1 + \left( \frac{z}{z_R} \right)^2 \right]^{1/2}, \quad (2.230)$$

and

$$R(z) = z \left[ 1 + \left( \frac{z_R}{z} \right)^2 \right], \quad (2.231)$$

where  $z_R$  is called the Rayleigh range. The Rayleigh range is the distance over which the cross section of the beam doubles. The Rayleigh range is related to the initial beam waist and the wavelength of light according to

$$z_R = \frac{\pi w_0^2}{\lambda}. \quad (2.232)$$

### Intensity

Figure 2.57 shows the intensity of the Gaussian beam according to Eq.(2.227) for different propagation distances.

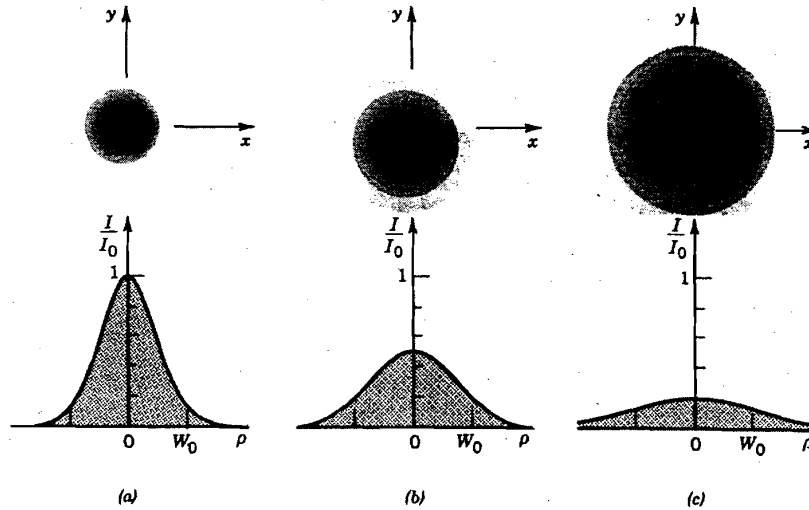


Figure 2.57: The normalized beam intensity  $I/I_0$  as a function of the radial distance  $r$  at different axial distances: (a)  $z=0$ , (b)  $z=z_R$ , (c)  $z=2z_R$ .

The beam intensity can be rewritten as

$$I(r, z) = I_0 \frac{w_0^2}{w^2(z)} \exp \left[ -\frac{2r^2}{w^2(z)} \right], \quad \text{with } I_0 = \frac{2P}{\pi w_0^2}. \quad (2.233)$$

For  $z > z_R$  the beam radius grows linearly and therefore the area expands quadratically, which brings down the peak intensity quadratically with propagation distance.

On the beam axis ( $r = 0$ ) the intensity is given by

$$I(r, z) = I_0 \frac{w_0^2}{w^2(z)} = \frac{I_0}{1 + \left( \frac{z}{z_R} \right)^2}. \quad (2.234)$$

The normalized beam intensity as a function of propagation distance is shown in Figure 2.58

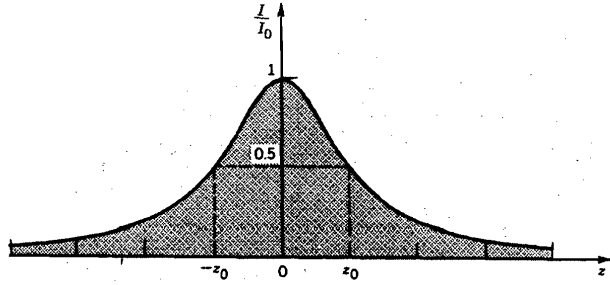


Figure 2.58: The normalized Beam intensity  $I(r = 0)/I_0$  on the beam axis as a function of propagation distance  $z$  [6], p. 84.

### Power

The fraction of the total power contained in the beam up to a certain radius is

$$\begin{aligned}
 \frac{P(r < r_0)}{P} &= \frac{2\pi}{P} \int_0^{r_0} I(r, z) r dr \\
 &= \frac{4}{w^2(z)} \int_0^{r_0} \exp\left[-\frac{2r^2}{w^2(z)}\right] r dr \quad (2.235) \\
 &= 1 - \exp\left[-\frac{2r_0^2}{w^2(z)}\right].
 \end{aligned}$$

Thus, there is a certain fraction of power within a certain radius of the beam

$$\frac{P(r < w(z))}{P} = 0.86, \quad (2.236)$$

$$\frac{P(r < 1.5w(z))}{P} = 0.99. \quad (2.237)$$

### Beam radius

Due to diffraction, the smaller the spot size at the beam waist, the faster the beam diverges according to 2.230 as illustrated in Figure ??.

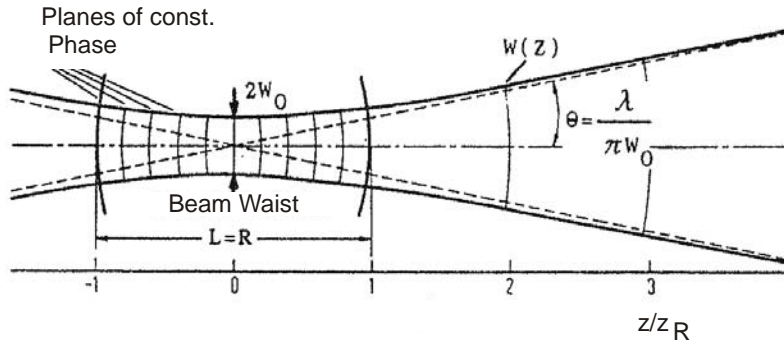


Figure 2.59: Gaussian beam and its characteristics.

### Beam divergence

The angular divergence of the beam is inversely proportional to the beam waist. In the far field, the half angle divergence is given by

$$\theta = \frac{\lambda}{\pi w_o}, \quad (2.238)$$

see Figure 2.59.

### Confocal parameter and depth of focus

In linear microscopy, only a layer which has the thickness over which the beam is focused, called depth of focus, will contribute to a sharp image. In nonlinear microscopy (see problem set) only a volume on the order of beam cross section times depth of focus contributes to the signal. Therefore, the depth of focus or confocal parameter of the Gaussian beam, is the distance over which the beam stays focused and is defined as twice the Rayleigh range

$$b = 2z_R = \frac{2\pi w_o^2}{\lambda}. \quad (2.239)$$

The confocal parameter depends linearly on the spot size (area) of the beam and is inverse to the wavelength of light. At a wavelength of  $1\mu m$  a beam with a radius of  $w_o = 1cm$ , the beam will stay focused over distances as long

600m. However, if the beam is strongly focussed down to  $w_o = 10\mu\text{m}$  the field of depth is only  $600\mu\text{m}$ .

### Phase

The phase delay of the Gaussian beam is

$$\Phi(r, z) = k_0 z - \zeta(z) + k_0 \frac{r^2}{2R(z)} \quad (2.240)$$

$$\zeta(z) = \arctan\left(\frac{z}{z_R}\right). \quad (2.241)$$

On beam axis, there is the additional phase  $\zeta(z)$  when the beam undergoes focussing as shown in Figure 2.60. This is in addition to the phase shift that a uniform plane wave already acquires.

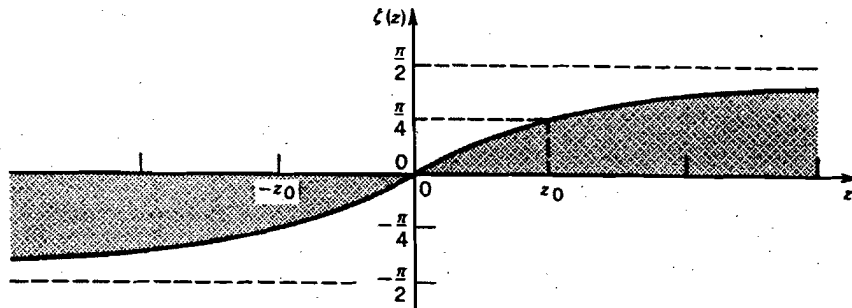


Figure 2.60: Phase delay of a Gaussian beam relative to a uniform plane wave on the beam axis [6], p. 87. This phase shift is known as Guoy-Phase-Shift.

This effect is known as Guoy-Phase-Shift. The third term in the phase shift is parabolic in the radius and describes the wavefront (planes of constant phase) bending due to the focusing, i.e. distortion from the uniform plane wave.



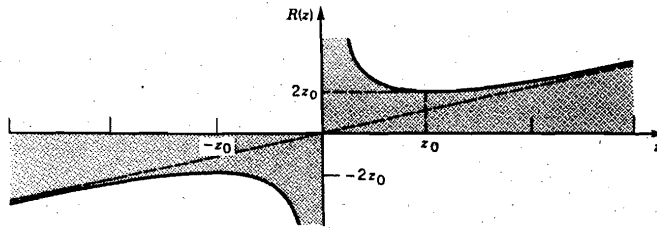


Figure 2.61: The radius of curvature  $R(z)$  of the wavefronts of a Gaussian beam [6], p. 89.

The surfaces of constant phase are determined by  $k_0 z - \zeta(z) + k_0 \frac{r^2}{2R(z)} = \text{const.}$  Since the radius of curvature  $R(z)$  and the additional phase  $\zeta(z)$  are slowly varying functions of  $z$ , i.e. they are constant over the radial variation of the wavefront, the wavefronts are paraboloidal surfaces with radius  $R(z)$ , see Figures 2.61 and 2.62.

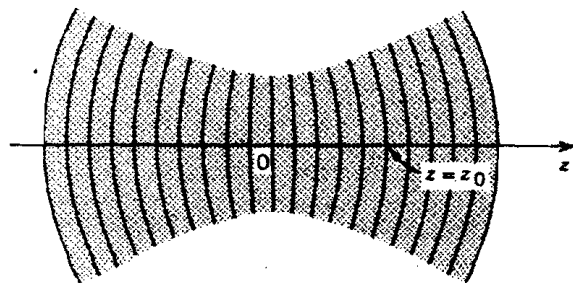


Figure 2.62: Wavefronts of a Gaussian beam, [6] p. 88.

For comparison, Figure 2.63 shows the wavefront of (a) a uniform plane wave, (b) a spherical wave and (c) a Gaussian beam. At points near the beam center, the Gaussian beam resembles a plane wave. At large  $z$ , the beam behaves like a spherical wave except that the phase fronts are delayed by a quarter of the wavelength due to the Guoy-Phase-Shift.

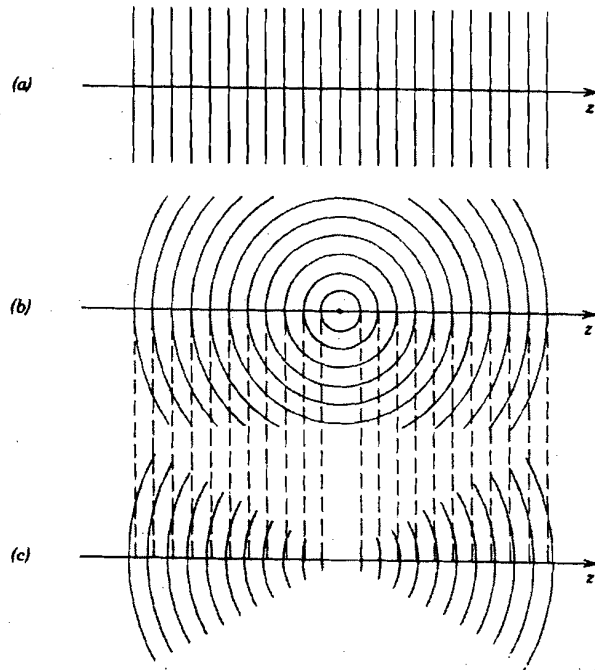


Figure 2.63: Wavefronts of (a) a uniform plane wave; (b) a spherical wave; (c) a Gaussian beam [5], p. 89.